Catalase Nanocapsules Protected by Polymer Shells for Scavenging Free Radicals of Tobacco Smoke

Lizhi Liu, Wei Yu, Dan Luo, Zhenjie Xue, Xiaoyun Qin, Xiaohua Sun, Jincai Zhao, Jianlong Wang, and Tie Wang**

Free radicals in tobacco smoke trigger numerous lung diseases, which are worldwide health considerations. The ideal free-radical, tobacco-smoke scavenger must be highly reactive and temperature resistant. Catalases (CATs) show attractive potential to scavenge free radicals in tobacco smoke, because of their higher reaction rate compared to that of non-catalyzed reactions. Their fragile nature, however, diminishes their catalytic activity in hot tobacco smoke. Therefore, it is essential to enhance the structural integrity and catalytic stability of these enzymes under severe environmental conditions. In order to improve the thermal stability of CATs, we have developed a facile approach to produce CAT nanocapsules (nCATs) by encapsulating a single enzyme in a polyacrylamide (PAAM) shell. The rigid polymer shells on the CATs surface prevents their free deformation. The secondary structure of the enzyme is retained and their dissociation is almost nil even under high operational temperatures. As a result, the structural stability and thermal resistance of the enzyme are significantly enhanced. The nCATs are covalently bound on cellulose acetate fibers to enable the enzyme sticking to the cigarette filters.The electron paramagnetic resonance (EPR) and Saltzman procedure reveal that the nCATs are able to efficiently scavenge 90% of the free radicals in tobacco smoke. The use of such nCATs with improved enzyme thermal stability opens up new opportunities for future application in cigarette filters.

1. Introduction

Tobacco is indeed a worldwide public health hazard whose significant morbidity and mortality figures, as well as its deleterious abusive effects are well known by the public.[1] Each smoked cigarette can generate at least 100 trillion free radicals that contain unpaired electrons in their atomic orbitals and are temporary unstable and highly reactive.[2] One of the things that makes smoking so dangerous lies in the fact that high concentrations of free radicals are accumulated in a fast way.[3] These free radicals severely damage lung tissue and compromise the body's immune defenses, which triggers a number of diseases, such as lung cancer and chronic obstructive pulmonary disease (COPD).[4] To minimize smoking-induced damage, the most common method nowadays to scavenge free radicals is adding antioxidants into the cigarette filter, such as lycopene, grape seed extract, pycnogenol, etc.[5] Considering the fact that tobacco smoke is a hot aerosol that quickly passes through the cigarette filter, the material used for eliminating free radicals should match two essential parameters: it must show a high reactivity and thermal resistance.

Very different from previous works, in which hemoglobin and heme-containing compounds were used to get rid of nitric oxide, reactive oxidants, and carcinogenic volatile nitroso compounds in tobacco smoke,[6] we report a new route to scavenge free radicals via catalase nanocapsules (nCATs), an encapsulated single enzyme in a polyacrylamide (PAAM) shell. It is the first time that visual evidence is provided of the fact that rigid polymer shells significantly improve the thermal stability of an enzyme against changes in its quaternary structure. Enzyme reaction rates are millions of times faster than those of comparable non-catalyzed reactions.[7] So catalases (CATs) show attractive potential to eliminate free radicals in tobacco smoke.[6b] However, their efficiencies have not been satisfactory because of their fragile nature under higher temperatures. Just 40% of free radicals were scavenged when native CATs were put into cigarette filters, because native CATs easily lose their activity in non-physiological

L. Z. Liu, Dr. W. Yu, D. Luo, Z. J. Xue, X. Y. Qin, Dr. X. H. Sun, Prof. T. Wang
Beijing National Laboratory for Molecular Sciences
Key Laboratory of Analytical Chemistry for Living Biosystems
Institute of Chemistry
The Chinese Academy of Sciences
#2 Zhongguancun North First Street
Beijing 100190, P.R. China
E-mail: wangtie@iccas.ac.cn

L. Z. Liu, Prof. J. L. Wang
College of Food Science and Engineering
Northwest A&F University
Yangling, 712100 Shaanxi, P.R. China
E-mail: wanglong79@yahoo.com

Prof J. C. Zhao
Beijing National Laboratory for Molecular Sciences
Key Laboratory of Photochemistry
Institute of Chemistry, The Chinese Academy of Sciences
#2 Zhongguancun North First Street
Beijing 100190, P.R. China

DOI: 10.1002/adfm.201501850

conditions, and the overall processes are accelerated by the high operational temperature. The applications of CATs are therefore still negligible and challenging. Therefore, developing an effective approach to stabilize CATs and retain their activity is crucial toward scavenging free radicals in tobacco smoke.

The reason of enzyme inactivation at high temperatures is that CATs dissociate into four subunits accompanied by a change in shape and structure.[8] Although there are many methods to protect CATs by encapsulating them in polymeric nanocarriers,[9] it is difficult to prevent CATs from dissociating because in a multiple enzyme vesicle there is always space for deformation of the CAT. To prevent the dissociation of the enzyme under high temperatures, we, therefore, encapsulated a single enzyme in a polyacrylamide (PAAM) shell. The rigid polymer shells provide the soft enzyme with rigidity and strength against mechanical stress to restrict morphogenesis and prevent over-expansion or dissociation.[10] The nCATs have two benefits for scavenging free radicals. Firstly, the enzyme motion is restricted in the nanocapsule. Because 26 out of 28 lysine groups on each CAT are firmly bound to the polymer shells via multipoint covalent linkage, dissociation of the CAT at high temperature is prevented. nCATs can retain their catalytic activity up to 65 °C for at least 60 min. As a result, the thermal resistance and heat stability are significantly enhanced, and up to 90% of free radicals could be cleaned when 1 mg of nCATs was put in cigarette filters. Secondly, the nCATs could be covalently fastened to the cellulose acetate fibers without decreasing their catalytic activity, thus preventing falling off of the nCATs from the cigarette filters by physical entrapment or deactivation of the covalent bond.[11] This points to future applications of nCATS in cigarette filters.

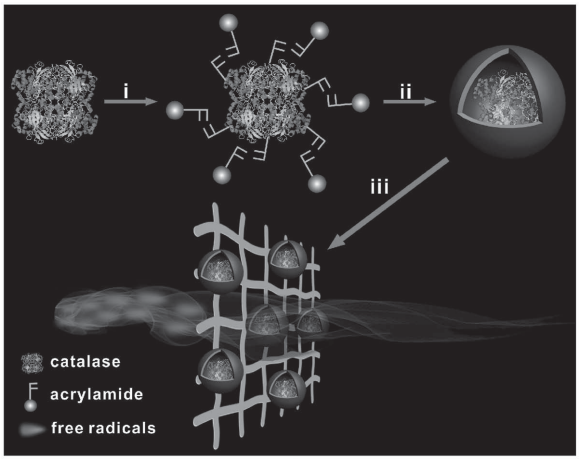

Scheme 1. Illustration of construction of nCATs for scavenging free radicals in tobacco smoke. Step i) CAT surfaces are conjugated with polymerizable acryl groups; step ii) polymer shells are generated by an in-situ polymerization of acrylamide; step iii) the cigarette filters are covalently bound to nCATs and offer a novel platform for scavenging free radicals in tobacco smoke. The structure of beef-liver catalase has been uploaded to the RCSB Protein Data Bank under the access code 8CAT.

2. Results and Discussion

2.1. Formation and Characterizations of nCATs

The synthesis of our nCATs followed a simple two-step process as illustrated in **Scheme 1**. Step i) the CATs were conjugated with polymerizable acryl groups via a reaction between the lysine groups and *N*-acryloxysuccinimide (NAS); step ii) subsequent polymerization allowed a thin polymer shell to grow around the conjugated CATs at room temperature. These polymer shells provided structural support and protection of the CATs against dissociation, whereby the interior osmotic environment of the CATs was retained, thereby affording exceptional activity and stability under high operational temperatures.

Various characterization techniques were performed to determine the formation of the nCATs. **Figure 1**a shows a representative atomic force microscopy (AFM) image of nCATs with a diameter of 18.2 ± 5.6 nm, which is consistent with the transmission electron microscopy (TEM) images. The nCATs exhibit a spherical morphology with a diameter of 17.7 ± 4.8 nm, and the polymer shells have a thickness of around 4.1 ± 0.5 nm (Figure 1b). Subtracting the size of the polymer shells, the nCAT core was estimated to be 9.5 ± 4.8 nm, which is comparable to the size of native CATs (9.0 nm × 6.0 nm × 2.0 nm).[12] This implied that each of the nCATs contained only a single enzyme in most cases. In order to further verify this viewpoint, dynamic light scattering (DLS) was employed to measure the size distribution and zeta potential of native CATs and nCATs (Figure 1c). Native CATs exhibit a negative charge (about –20 mV, Figure S1 in the Supporting Information) with a size distribution centered at 9.1 nm. For comparison, the size distribution of nCATs was 20.2 nm suggesting the successful encapsulation of a single enzyme in a polymer shell. As the polymer shells were synthesized by polymerizing a neutral monomer of

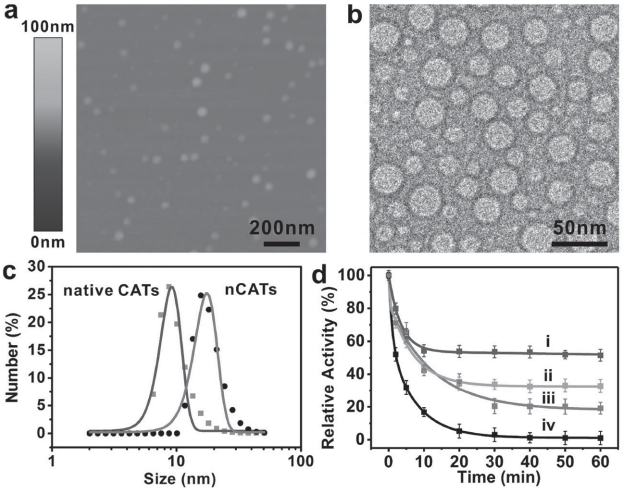

Figure 1. a,b) Representative AFM (a) and TEM (b) images showing that the nCATs have spherical morphologies. c) DLS measurements revealing the size distribution of native CATs and nCATs. d) Thermal resistance and heat stability under operational temperature of 65 °C of nCATs prepared at various NAS/CAT molar ratios: i) 500:1, ii) 300:1, iii) 100:1, and iv) native CATs.

acrylamide (AAM), the nCATs showed a smaller negative charge (about –10 mV, Figure S1 in the Supporting Information) than the native CATs. Successful encapsulation was also validated by Fourier-transform infrared (FTIR) spectra (Figure S2 in the Supporting Information), whereby the nCATs showed characteristic absorption peaks at 3350 cm^{-1} (N–H stretching), 1630 cm^{-1} (NH_2 bending), and 1450 cm^{-1} (C–N stretching), all of which could be ascribed to the PAAM shells of the nCATs.

2.2. Catalytic Activity of nCATs

A significant reduction in enzyme activity has often been observed when enzyme are immobilized or encapsulated. This decrease in activity can mainly be attributed to two challenges: steric hindrance and mass transport resistance. Table S1 in the Supporting Information lists the activities of native CATs and nCATs, as determined by the method described in the Experimental section. It can be seen that the nCATs retain 85% of the specific activity of the native CATs. One advantage of the present procedure is that the encapsulated enzymes can maintain their secondary structure, as represented in the circular dichroism spectra (CD) in the Supporting Information (Figure S3). Another advantage is that the enzymes are provided with good accessibility to their substrates, which is confirmed by the catalytic efficiency of the enzymes. Generally, enzyme immobilization also leads to a significant decrease in catalytic efficiency (k_{cat}/K_m), because of a decrease in the turnover number (k_{cat}) and an increase of the Michaelis constant (K_m).[13] However, in our case, the nCATs exhibited an upward trend in catalytic efficiency (Figure S4 in the Supporting Information), slightly increasing from $5.33 \pm 0.06 \times 10^5$ $M^{-1}S^{-1}$ to $7.86 \pm 0.54 \times 10^5$ $M^{-1}S^{-1}$, because the k_{cat} of the nCATs is roughly 4.9 times higher than that of the native CATs, which is accompanied by a rise in K_m value of about 3.3 times. The enhancement in catalytic efficiency may be related to the increase in collision frequency between the substrate and the enzyme. The collision frequency has been shown to increase dramatically as the size of the polymer shell decreases.[14] This implies that, in our case, the reaction probability between the enzyme and the substrate has increased. The rate constants involved in enzyme–substrate complex formation and reaction to the product are affected to a different extent by the encapsulation as a whole. The thermal endurance of the catalytic activity was also significantly improved by the encapsulation of the CATs in the polymer shells. The deactivation curves of native CATs and nCATs, which were both incubated at 65 °C at different NAS/CAT molar ratios (100:1, 300:1, and 500:1), are demonstrated in Figure 1d. The native CATs show a distinctly fast and continuous slope of activation loss (total inactivity after 60 min), whereas the nCATs undergo a slower decrease in catalytic activity in the first 20 min, and they maintain at least 20% of the original activity for 60 min under all measuring conditions. The nCATs, thus, possess a much better thermal stability, which may be related to the multiple covalent attachments between the enzyme and the polymer shell, which effectively hinders conformational changes in the CATs when heated. As expected, the higher the NAS/CAT ratio, the better the thermal stability is. However, the catalytic activity significantly decreases if the ratio of NAS/CAT is higher than 500:1 (Figure S5a in the Supporting Information). From these thermal stability and activity assays, an optimal NAS/CAT molar ratio of 500:1 was selected as the basic condition for the following experiments. We also discovered that the nCATs retained around 90% of their original activity even after storage for 10 weeks at 8 °C, whereas the native CATs lost most of their activity within 2 weeks under similar storage conditions (Figure S5b in the Supporting Information). As the nCATs were formed by polymerizing acrylamides around the surface of the CATs, the acrylamides may replace the hydrogen bonds between the enzymes and their bound water. If there bound water is still present after drying, molecular motion of the enzymes is possible, which facilitates conformational changes and consequently leads to inactivation. Therefore encapsulating CATs in polymer capsules raises the decomposition temperature of the enzymes (Figure S6 in Supporting Information), which is desirable for long-term storage.[8c]

2.3. Thermal Stability of nCAT

CATs from many species are known as tetramers with molecular weights of 60 to 75 kDa. The Heme groups are their active sites, which are buried deep within the subunits that contain an eight-stranded β-barrel, and an α-helical domain.[15] These different subunits are hooked together by wrapping a loop around the *N*-terminal of the α-helical.[16] High operational temperatures significantly disrupt the α-helical of native CATs, resulting in the dissociation into subunits of the tetrameric enzyme. The native CATs are then divided into four domains and these subsequently release Fe^{3+} ions from their heme prosthetic groups. To prevent this over-expansion of our CATs and to retain a stable osmotic environment, as well as the quaternary structure, the polymer shells were used as pressure vessels. The enhanced thermal stability of the nCATs can also account for their structural stability (**Figure 2**a). The structural stabilities of native CATs and nCATs were characterized by CD and UV–vis spectra. The CD spectra for both types of CATs show two main negative bands at 210.5 and 219.5 nm (Figure S3 in the Supporting Information), which are characteristic of the α-helical structure of the enzyme, and are in accordance with the $\pi \rightarrow \pi^*$ and $n \rightarrow \pi^*$ amide transitions of the polypeptide chain, respectively.[17] The presence of adjacent α-helical structures with an antiparallel arrangement has been shown to have positive effects on protein stability.[18] After treatment at 65 °C for 30 min, the changes in the secondary structure of the native CATs and nCATs were monitored, as shown in Figure 2b. For native CATs, the two negative bands at 210.5 and 219.5 nm were significantly altered. Especially, the ellipticity at 219.5 nm almost disappeared. For comparison, the shape of the bands for the nCATs remained the same although the band at 219.5 nm had red-shifted by 3 nm. These results indicate that the high operational temperature disrupts the α-helical conformation of native CATs, but has a negligible effect on the structural integrity of nCATs.

The Soret band reflects the $\pi \rightarrow \pi^*$ transition of the heme porphyrin ring, which is very sensitive to variations in the microenvironment around the heme prosthetic group (Figure S7 in the Supporting Information).[19] As previously

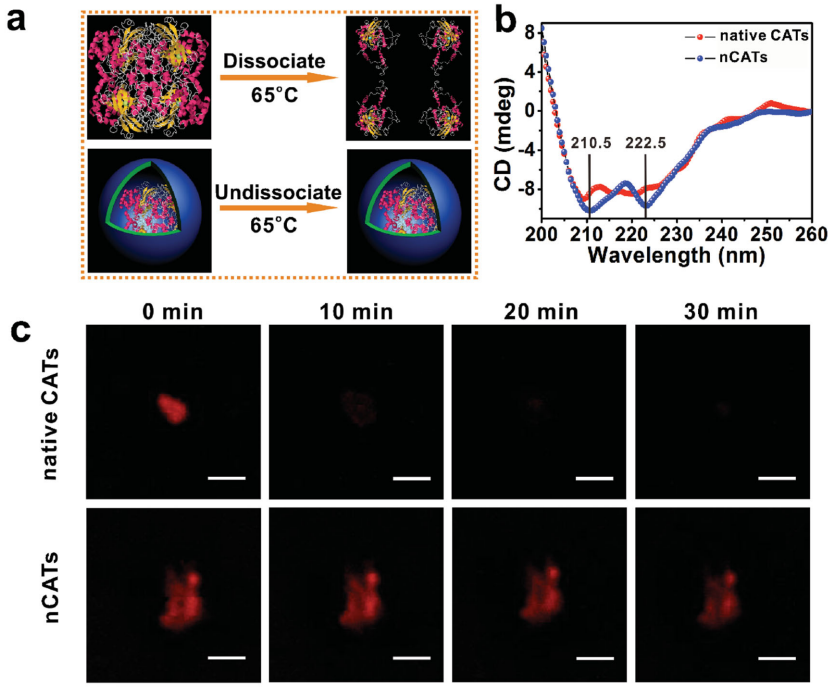

Figure 2. a) Schematic exhibiting dissociation of native CATs into subunits and nCATs retaining their structural integrities under high operational temperature. b) CD spectra demonstrating the secondary structures of native CATs and nCATs incubated at 65 °C for 30 min. c) Fluorescence changes in native CATs and nCATs as a function of incubating time at 65 °C. Scale bar is 10 μm.

reported, the changes in the Soret band region are closely related to the CAT dissociation process.[20] A large decrease in extinction coefficient at 410 nm in the UV–vis spectra thus relates to the splitting of the enzyme and the breakage of the heme–protein bond.[21] Under thermal induction, the subunit–subunit interactions become weaker, and native CATs tend to dissociate. For the nCATs, however, the thermal treatment leads to a negligible decrease in absorbance, indicating a stabilization of the porphyrin microenvironment. The number of acryloyl groups on each enzyme are listed in Table S2 (Supporting Information). Because 26 out of the 28 lysine groups of a single CAT are bound to the polymer shell via multipoint covalent linkages,[22] the mobility of the enzyme is restricted, which prevents the CATs from dissociating into subunits.

In order to further confirm this viewpoint, rhodamine-B-labeled CATs (CATs–Rhb) and rhodamine-B-labeled nCATs (nCATs–Rhb) were incubated at 65 °C, and observed by fluorescence microscopy. (Note: nCATs-Rhb were prepared by first conjugating the CATs with rhodamine-B, followed by the same polymer shell coating process as for nCATs). As shown in Figure 2c, the fluorescence of the CATs–Rhb significantly decreased after 10 min and disappeared after about 30 min. Because of the tetrameric enzyme dissociation into subunits, the Fe^{3+} ions of the heme porphyrin buried within the CATs was released. These Fe^{3+} ions led to the fluorescence quenching of rhodamine-B. In contrast, the nCATs–Rhb retained their structural integrity because of their protection by the polymer shells. Therefore, the fluorescent intensity did not change after incubation.

Furthermore, the thermal properties of native CATs and nCATs were investigated by thermogravimetry (TG), as shown in Figure S6 in the Supporting Information. Native CATs revealed two main thermal decomposition steps. The first weight loss occurred at around 100 °C, which can mainly be contributed to water evaporation. The second weight loss started at about 300 °C, which is caused by the decomposition of the CATs. Compared to this, the nCATs showed three weight-loss steps as a function of temperature. The first one can again be associated with water evaporation, whereas the other two can be assigned to the decomposition of the PAAM shells and that of the enzymes, respectively. The PAAM shells started to decompose at 220 °C. Because of their protective polymer shells, the decomposition temperature of the CATs themselves was increased to 360 °C. Therefore we can conclude that nCATs exhibit a much better thermal stability.

2.4. Scavenging Free Radicals in Tobacco Smoke

Free radicals produced in tobacco smoke were analyzed by electron paramagnetic resonance (EPR). Tobacco smoke was generated and collected as shown in **Figure 3**a. *N*-tert-butyl-2-phenyl nitrone (PBN) was used as the spin-trapping agent, the nCATs were used as free-radical scavengers. For safety reasons, the nCATs must be stably secured in the cigarette filters, especially at the end of the mouthpiece. The cigarette filters were made with cellulose acetate fibers possessing carboxylic groups, which was confirmed by FTIR. The characteristic absorption peak for the C=O stretching was observed at 1760 cm^{-1} (Figure S8, Supporting Information). Through reactions between the carboxylic groups of cellulose acetate fibers and the amine groups of polymer shells, nCATs are able to covalently attach to the cigarette filters (**Figure 4**a). The cellulose acetate fibers were incubated in nCAT solution with or without 1-ethyl-3-(3-dimethylaminopropyl)carbodiimide/*N*-hydroxysuccinimide (EDC/NHS) for 2 h. After extensive washing for three times, the surface morphologies were analyzed by scanning electron microscopy (SEM, Figure 3b,c). In the absence of EDC/NHS, the surface of the cellulose acetate fibers was smooth and neat. In the presence of EDC/NHS, on the other hand, the cellulose acetate fibers presented a rough surface, which implies that the nCATs were successfully loaded onto the surface of the cigarette filters. To demonstrate this concept more clearly, the nCATs were replaced by nCATs-Rhb. After physical entrapment of the nCATs-Rhb, the fluorescence on the fibers disappeared rapidly after subsequent washing processes (Figure 4bi). On the contrary, when nCATs-Rhb were covalently bound to the fibers, intensive fluorescence could still be seen even after extensive washing (Figure 4bii). The fluorescence microscopy thus demonstrates that the nCATs were successfully loaded on

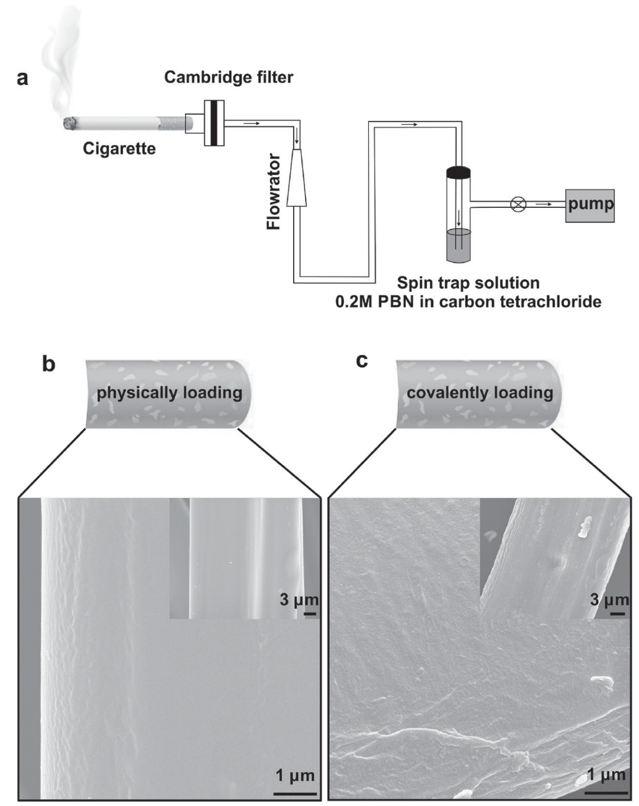

Figure 3. a) A diagram of the smoking-simulation set-up for collecting free radicals from tobacco smoke. b,c) SEM images of nCATs-cellulose acetate fibers generated by physical entrapment (b) and covalent seizing (c), after extensive washing for three times.

the cigarette filters, and the covalent binding provided a more stable performance, which is a major improvement for practical applications.

The cigarette filters covalently bound by nCATs were then used to evaluate their scavenging capacity against free radicals in tobacco smoke. Taking away the weight of the 12.9% PAAM shells (Figure S9, Supporting Information), we estimated that approximately 1.0 mg of enzyme was used each time. We quantified this by measuring the concentration of the initial and that of the residual enzyme solution (Figure S10 in the Supporting Information). An equivalent amount of native CATs was physically absorbed on the cigarette filters for comparison. Tobacco smoke of a single cigarette was bubbled through 2.0 mL trapping solution to yield EPR spectra (Figure 4c). The test system was sealed to insure that the relative concentration of free radicals generated was identical for every cigarette. The cigarette tar was filtered using Cambridge filters. The free radicals generated by smoked cigarettes are usually nitric oxide (NO•), alkoxyl (RO•), alkyl (R•), and alkylperoxide (ROO·) radicals.[23] It is well known that CATs facilitate the two-step decomposition of hydrogen peroxide (H_2O_2) (Equation S1, S2 in the Supporting Information), and show a preferential peroxidatic activity towards small substrates like NO (Equation S3, Supporting Information).[24] The ability of nCATs for scavenging free radicals from tobacco smoke involves a series of processes:[25] 1) NO slowly oxidizes to reactive nitrogen dioxide (Equation (1); 2) this nitrogen dioxide reacts with an unsaturated compound, such as isoprene, to form a carbon-centered radical (abbreviated as R• in Equation (2); 3) the carbon radical rapidly reacts with dioxygen to form a peroxyl radical (Equation (3); 4) as in smog, the peroxyl radical is then converted to an alkoxyl radical by reaction with NO (Equation (4)), producing more nitrogen dioxide.[26]

$$NO + 1/2O_2 \rightarrow NO_2 \quad (1)$$

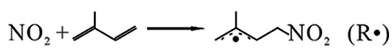

(2)

$$R\bullet + O_2 \rightarrow ROO\bullet \quad (3)$$

$$ROO\bullet + NO \rightarrow RO\bullet + NO_2 \quad (4)$$

The EPR signal intensity is proportional to the relative concentration of free radicals (Figure 4c). It can be seen that the blank cigarette filters and even the cigarette filters with physically absorbed 0.15 mg PAAM polymer were not able to inactivate the free radicals in the tobacco smoke. Compared to blank cigarette filters, the cigarette filters filled with native CATs do also not reveal a significant reduction, although 32% of the enzymes retained their catalytic activity even after purging with hot smoke for 5 min. However, in the nCATs about 63% of the enzymes remained active under the same conditions, because the thermal stability of the enzymes was improved by the polymer shells (Figure S11, Supporting Information). The efficacy of nCATs in the cigarette filters is therefore also very

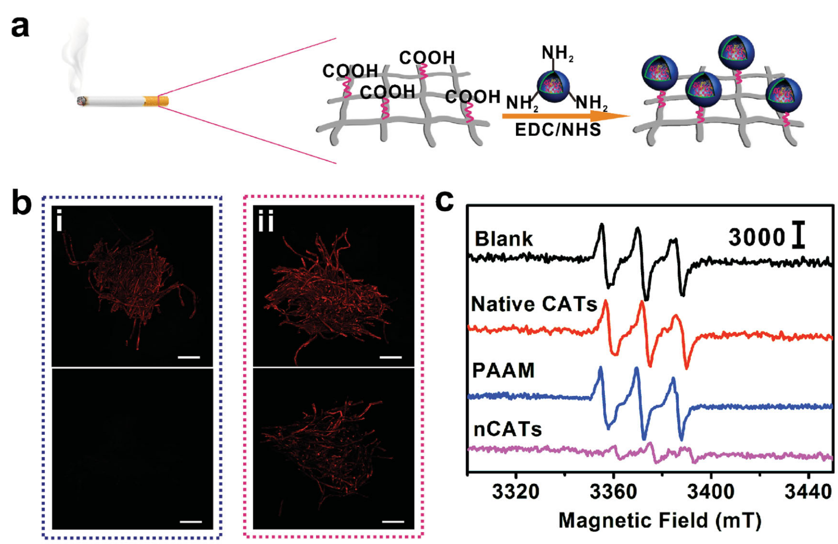

Figure 4. a) Scheme showing the immobilization of the nCATs in the cigarette filters. b) Confocal microscopy fluorescent images comparing i) physical absorption, and ii) covalent linkage of nCATs-Rhb onto the cellulose acetate fibers before (upper) and after (bottom) extensive washing for three times. Scale bar is 100 μm. c) EPR spectra of the spin-trapping solution (0.2 M PBN in carbon tetrachloride, 2.0 mL) bubbled with tobacco smoke of a single burning cigarette.

significant. Only around 10% of the free radicals survive after going through the cigarette filters containing the nCATs. The EPR spectrum shows an extremely low signal intensity, indicating that nCATs are efficient scavengers against free radicals in the gas phase. The quantitative analysis of one of the major radicals in cigarette smoke, nitric oxide, was further determined using the Saltzman procedure. The data obtained from the Saltzman procedure was a little lower than the values obtained by EPR. Only 6.85% NO_x was left after treatment with the nCATs scavenger (Figure S12 and S13 in the Supporting Information). This may be attributed to two factors: first, the nCATs possess a high thermal stability in hot smoke. Second, the nCATs have a higher catalytic efficiency than native CATs because of the increase in collision frequency between the substrate and the enzyme. This means that nCATs may be beneficial to capture free radicals in tobacco smoke. Only 1 mg of nCATs was able to scavenge up to 90% of free radicals in tobacco smoke. Such high scavenging capacity may stimulate future applications of nCATs in commercial cigarette filters to reduce smoking-generated mutagens in humans.

3. Conclusion

We have demonstrated a novel approach to prepare robust and highly active nCATs by a two-step in-situ polymerization in aqueous solution. The multipoint covalent linkage between the enzyme and the rigid polymer shells enables the nCATs to reproduce the catalytic properties of native CATs in their free form. The structural stability and thermal resistance were significantly strengthened to effectively inhibit the dissociation of CATs at high temperature. In addition, 90% of free radicals in tobacco smoke could be eliminated by cigarette filters containing nCATs. As the cigarette filters with nCATs possess a commendable biological activity and are harmless to human health, these findings may shed new light on the synthesis of enzyme nanocapsules as well as their use in industry applications.

4. Experimental Section

Preparation of nCATs: A volume of 10 mg CATs in 3.8 mL of phosphate buffer (pH 7.0, 50 mM) was reacted with 3.5 mg *N*-acryloxysuccinimide (NAS) in 300 µL dimethyl sulfoxide (DMSO) for 2 h at room temperature. The solution was then thoroughly dialyzed against pH 7.0 with a 50 mM phosphate buffer using a dialysis tubing membrane (MWCO = 3500 kDa, Solarbio Co.) to remove any unreacted NAS. Using 5 mL acryloylated CAT solution (1 mg mL^{-1}), radical polymerization of the surface of the acryloylated CATs was initiated by adding 6 mg ammonium persulfate dissolved in 30 µL deoxygenated and deionized water and 15 µL *N*,*N*,*N*′,*N*′-tetramethylethylenediamine into the test tube. Next, a specific amount of acrylamide and *N*,*N*′-methylene bisacrylamide (molar ratio = 6:1) dissolved in 0.5 mL of deoxygenated and deionized water was added to the test tube over 60 min. The reaction was allowed to proceed for another 60 min in a nitrogen atmosphere. Finally, dialysis was used to remove unreacted monomers and initiators.

Synthesis of nCATs-Cellulose Acetate Nanocomposites: Cellulose acetate (CA) was obtained from cigarette filters. CA was covalently linked with nCATs through the 1-ethyl-3-(3-dimethylaminopropyl)carbodiimide/*N*-hydroxysuccinimide (EDC/NHS) reaction. EDC and NHS were dissolved in 4 mL (1 mg mL^{-1}) nCATs at a concentration of 50 mM and 5 mM, respectively. Then, the CA was left to incubate in the above solution for 4 h at 4 °C. Unreacted nCATs, EDC, and NHS were removed by extensive washing in deionized water. The nCATs-CA nanocomposites were then freeze-dried for further use. The amount of nCATs loaded on the CA was determined by measuring the enzyme concentration in the initial and residual nCATs solutions.

Preparation of Cigarette Smoke and Analysis of Free Radicals: All research cigarettes were provided by China Tobacco Jiangxi Industrial Corp. Ltd., Jiangxi, P. R. China. The smoking simulation for routine analysis was performed at ambient temperature using a single-port smoking device (Figure 3a). Prior to the smoking simulation, the research cigarettes were unpacked and kept in a constant-humidity environment (20 °C, 60% relative humidity). For the simulation the research cigarettes were "smoked" with the velocity of the flue gas set at 40 mL min^{-1}. For each experiment, a single cigarette was taken for free-radical analysis. The gas-phase free radicals were collected by passing cigarette smoke from the main stream through a Cambridge filter pad, after which the smoke was introduced into a spin-trapping solution (0.2 M *N*-tert-butyl-2-phenyl nitrone (PBN) in carbon tetrachloride, 2.0 mL). After the last puff, the bubbled trapping solution was readjusted to its initial volume (2.0 mL) with carbon tetrachloride and a 200 µL aliquot was transferred into the EPR cell for spectral measurements.

EPR Analysis: EPR spectroscopy was performed using a Bruker E500–10/12: ELEXSYS EPR spectrometer operating in X-band mode (9.488 GHz) at a modulation frequency of 100 KHz. The spectrometer settings were: modulation amplitude, 0.0002 G; microwave, 10.1 mW and time constant, 40.96 ms for a sweep width of 400 G. The spectra are displayed as the first derivative of the EPR signals, which were recorded and digitized using a microprocessor and commercial software supplied by Bruker (UK). The hyperfine splitting constants applied throughout the analysis of the PBN adducts were determined from the simulated spectrum of the best-resolved signals. The relative scavenging rate (*E*) was calculated by:

$$E = \{(H_0 - H_X)/H_0\} \times 100\% \quad (5)$$

where H_0 and H_X are the integrated areas of the EPR peaks without and with scavenger, respectively.

Supporting Information

Supporting Information is available from the Wiley Online Library or from the author.

Acknowledgements

This research was financially supported by the 1000 Young Talents program, the National Natural Science Foundation of China (Grant Nos. 21422507, 21321003) and ICCAS. J.L. Wang appreciates the financial support from the New Century Excellent Talents in University (No. NCET-13–0483) and the Fundamental Research Funds of the Northwest A&F University of China (No. 2014YB093).

Received: May 5, 2015
Revised: June 7, 2015
Published online: July 14, 2015

[1] a) A. Csordas, D. Bernhard, *Nat. Rev. Cardiol.* **2013**, *10*, 219; b) V. Lobo, A. Patil, A. Phatak, N. Chandra, *Pharmacogn. Rev.* **2010**, *4*, 118.

[2] a) A. L. Bluhm, J. Weinstein, J. A. Sousa, *Nature* **1971**, *229*, 500; b) W. A. Pryor, *Environ. Health Persp.* **1997**, *105*, 875; c) M. Valko, D. Leibfritz, J. Moncol, M. Cronin, M. T. D. Mazur, J. Telser, *Int. J. Biochem. Cell. Biol.* **2007**, *39*, 44.

[3] a) S. S. Hecht, *Nat. Rev. Cancer* **2003**, *3*, 733; b) *The Chemical Components of Tobacco and Tobacco Smoke* (Eds: A. Rodgman, T. A. Perfetti), CRC Press, Boca Raton, FL, USA **2013**; c) P. Wan, X. D. Chen, *ChemElectroChem*. **2014**, *1*, 1602.
[4] a) M. Sopori, *Nat. Rev. Immunol*. **2002**, *2*, 372; b) M. R. Staempfli, G. P. Anderson, *Nat. Rev. Immunol*. **2009**, *9*, 377; c) Y. D. Liu, X. G. Han, L. He, Y. D. Yin, *Angew. Chem. Int. Ed*. **2012**, *51*, 6373.
[5] a) X. Shen, K. J. Zhong, X. J. Sun, H. B. Lu, Y. Shen, L. X. Yu, *Anal. Lett*. **2010**, *43*, 446; b) D. L. Zhang, Y. Tao, J. T. Gao, C. N. Zhang, S. J. Wan, Y. X. Chen, X. Z. Huang, X. Y. Sun, S. J. Duan, F. Schonlau, P. Rohdewald, B. L. Zhao, *Toxicol. Ind. Health* **2002**, *18*, 215.
[6] a) B. K. Vainshtein, W. R. Melik-Adamyan, V. V. Barynin, A. A. Vagin, A. I. Grebenko, *Nature* **1981**, *293*, 411; b) X. Lu, Z. Z. Hua, G. C. Du, X. L. Ma, J. H. Ca, Z. P. Yang, J. Chen, *Free Radical Res*. **2008**, *42*, 244; c) G. Deliconstantinos, V. Villiotou, J. C. Stavrides, *Anticancer Res*. **1993**, *14*, 2717; d) *Cigarette Smoke and Oxidative Stress* (Eds: B. B. Halliwell, H. E. Poulsen), Springer, Berlin, Germany **2003**; e) X. G. Hu, C. W. Wei, J. J. Xia, I. Pelivanov, M. O'Donnell, X. H. Gao, *Small* **2013**, *9*, 2046.
[7] a) Y. Liu, J. J. Du, M. Yan, M. Y. Lau, J. Hu, H. Han, O. O. Yang, S. Liang, W. Wei, H. Wang, J. M. Li, X. Y. Zhu, L. Q. Shi, W. Chen, C. Ji, Y. F. Lu, *Nat. Nanotech*. **2012**, *8*, 187; b) F. Y. Wang, Z. Liu, B. Wang, L. H. Feng, L. B. Liu, F. T. Lv, Y. L. Wang, S. Wang, *Angew. Chem. Int. Ed*. **2014**, *53*, 424; c) M. Yan, J. Ge, Z. Liu, P. K. Ouyang, *J. Am. Chem. Soc*. **2006**, *128*, 11008.
[8] a) B. Andreas, P. Sven, B. Matthias, *Angew. Chem. Int. Ed*. **2013**, *52*, 9673; b) C. Vieille, G. J. Zeikus, *Microbiol. Mol. Biol. Res*. **2001**, *65*, 1; c) N. J. Nosworthy, D. R. McKenzie, M. M. Bilek, *Biomacromolecules* **2009**, *10*, 2577.
[9] a) E. A. Simone, T. D. Dziubla, F. Colon-Gonzalez, D. E. Discher, V. R. Muzykantov, *Biomacromolecules* **2007**, *8*, 3914; b) E. D. Hood, M. Chorny, C. F. Greineder, I. S. Alferiev, R. J. Levy, V. R. Muzykantov, *Biomaterials* **2014**, *35*, 3708; c) T. D. Dziubla, A. Karim, V. R. Muzykantov, *J. Controlled Release* **2005**, *102*, 427; d) T. D. Dziubla, V. V. Shuvaev, N. K. Hong, B. J. Hawkins, M. Madesh, H. Takano, E. Simone, M. T. Nakada, A. Fisher, S. M. Albelda, V. R. Muzykantov, *Biomaterials* **2008**, *29*, 215; e) E. A. Simone, T. D. Dziubla, D. E. Discher, V. R. Muzykantov, *Biomacromolecules* **2009**, *8*, 1324; f) E. A. Simone, T. D. Dziubla, E. Arguiri, V. Vardon, V. V. Shuvaev, M. Christofidou-Solomidou, V. R. Muzykantov, *Pharm. Res*. **2009**, *26*, 250; g) M. Chorny, E. Hood, R. J. Levy, V. R. Muzykantov, *J. Controlled Release* **2010**, *146*, 144.
[10] a) O. I. Vinogradova, O. V. Lebedeva, B.-S. Kim, *Annu. Rev. Mater. Res*. **2006**, *36*, 143; b) M. Delcea, S. Schmidt, R. Palankar, P. A. Fernandes, A. Fery, H. Mohwald, A. G. Skirtach, *Small* **2010**, *6*, 2858; c) M. P. Neubauer, M. Poehlmann, A. Fery, *Adv. Colloid Interface Sci*. **2014**, *207*, 65.
[11] G. Deliconstantinos, V. Villiotou, J. C. Stavrides, *Anticancer Res*. **1994**, *14*, 2717.
[12] J. D. Zhang, Q. J. Chi, B. L. Zhang, S. J. Dong, E. K. Wang, *Electroanal*. **1998**, *10*, 738.
[13] a) L. Cao, *Curr. Opin. Chem. Biol*. **2005**, *9*, 217; b) A. M. Yashchenok, M. Delcea, K. Videnova, E. A. Jares-Erijman, T. M. Jovin, M. Konrad, H. Mohwald, A. G. Skirtach, *Angew. Chem. Int. Ed*. **2010**, *49*, 8116.
[14] Q. Chen, H. Schonherr, G. J. Vancso, *Small* **2009**, *5*, 1436.
[15] J. M. Wood, N. C. J. Gibbons, B. Chavan, K. U. Schallreuter, *Exp. Dermatol*. **2008**, *17*, 366.
[16] S. A. Costa, T. Tzanov, A. Filipa Carneiro, A. Parr, G. M. Gubitz, A. Cavaco-Paulo, *Enzyme Microbial Technol*. **2002**, *30*, 387.
[17] X. L. Wei, Z. Q. Ge, *Carbon* **2013**, *60*, 401.
[18] F. Secundo, *Chem. Soc. Rev*. **2013**, *42*, 6250.
[19] B. D. Abraham, M. Sono, O. Boutaud, A. Shriner, J. H. Dawson, A. R. Brash, B. J. Gaffney, *Biochemistry* **2001**, *40*, 2251.
[20] S. Prajapati, V. Bhakuni, K. R. Babu, S. K. Jain, *Eur. J. Biochem*. **1998**, *255*, 178.
[21] C. Tanford, R. Lovrien, *J. Am. Chem. Soc*. **1962**, *84*, 1892.
[22] a) J. Kim, J. W. Grate, *Nano Lett*. **2003**, *3*, 1219; b) W. Wei, J. Du, J. Li, M. Yan, Q. Zhu, X. Jin, X. Y. Zhu, Z. M. Hu, Y. Tang, Y. F. Lu, *Adv. Mater*. **2013**, *25*, 2212.
[23] *Molecular Interventions in Lifestyle-Related Diseases* (Eds: M. Hiramatsu, T. Yoshikawa, L. Packer), CRC Press, Boca Raton, FL, USA **2006**.
[24] a) T. J. Reid, M. R. Murthy, A. Sicignano, N. Tanaka, W. D. Musick, M. G. Rossmann, *Proc. Natl. Acad. Sci. USA* **1981**, *78*, 4767; b) F. Yan, S. Williams, G. D. Griffin, R. Jagannathan, S. E. Plunkett, K. H. Shafer, T. Vo-Dinh, *J. Environ. Monitor*. **2005**, *7*, 681; c) L. Brunelli, V. Yermilov, J. Beckman, *Free Radical Biol. Med*. **2001**, *30*, 709.
[25] a) W. A. Pryor, M. Tamura, D. F. Church, *J. Am. Chem. Soc*. **1984**, *106*, 5073; b) W. A. Pryor, K. Stone, *Ann. NY Acad. Sci*. **1993**, *686*, 12.
[26] D. F. Church, W. A. Pryor, *Environ. Health Persp*. **1985**, *64*, 111.